Control of Atomic Collisions by Laser Polarization

T. Schmidt,[1] C. Figl,[1] A. Grimpe,[1] J. Grosser,[1] O. Hoffmann,[1] and F. Rebentrost[2]
[1]*Institut für Atom- und Molekülphysik, Universität Hannover, 30167 Hannover, Germany*
[2]*Max-Planck-Institut für Quantenoptik, 85748 Garching, Germany*
(Received 2 August 2003; published 22 January 2004)

Atomic collision pairs in a light field form a microscopic interferometer. The light acts as the beam splitter and controls at the same time the amplitudes and phases of the interfering waves. We demonstrate the complete tunability using linear and elliptic polarization.

DOI: 10.1103/PhysRevLett.92.033201 PACS numbers: 34.50.Rk, 32.80.Qk, 39.20.+q

Angle-resolved cross sections of atomic collisions frequently show interference structures like Stueckelberg oscillations [1] or supernumerary rainbows [2]. They are an invariable manifestation of the collisional interactions. Atomic collisions in laser fields show analogous structures. The interaction with the light, however, allows manipulation of the collision in a controllable fashion.

The control of atomic and molecular processes by laser light is an active field of research. Coherent control [3,4] emphasizes the importance of the relative phase of the spectral components. Pulse shaping techniques and learning algorithms provide optimized electric field shapes [5–7], by which control of unimolecular processes was demonstrated. Control schemes involving collisions in caging reactions [8,9], ultracold gases [10], and bimolecular processes [11,12] show the high potential of the method. Laser polarization as a control tool [10,12,13] gains increased attention [6,14].

Macroscopic atom interferometers [15] exploit the wave nature of matter. They have found practical applications, e.g., in the rotation sensing Sagnac gyroscope [16] or for measuring forward scattering amplitudes [17]. Because of the small de Broglie wavelength, their potential sensitivity exceeds that of the corresponding optical devices by several orders of magnitude. Macroscopic Mach-Zehnder-type atom interferometers using light as the beam splitter show a remarkable similarity with the present microscopic interferometer. The linear dimensions of the two devices differ typically by a factor of 10^8, and even miniaturized atom interferometers [18] are a factor of 10^6 larger than the collisional interferometer discussed here.

We study here the optical excitation of transient NaNe collision pairs, i.e., the optical collision

$$\mathrm{Na}(3s) + \mathrm{Ne} + h\nu \rightarrow \mathrm{Na}(3p) + \mathrm{Ne}.$$

The differential cross section shows a regular oscillation structure reflecting the interference between two different pathways for the atomic wave during the collision. Using the polarization properties of the light field, we demonstrate complete control over the relative phase and amplitude of the individual contributions.

The process is most easily discussed in terms of a dressed collision pair model. In Fig. 1(a) the NaNe interaction energies in the presence of a light field, i.e., $U_{X\Sigma}(r) + h\nu$ and $U_{B\Sigma}(r)$, are shown as a function of the atom-atom distance r. Optical excitation is possible at the crossing (Condon) radius r_c where

$$U_{X\Sigma}(r_c) + h\nu = U_{B\Sigma}(r_c). \quad (1)$$

For the present purpose, a semiclassical approach [19] is appropriate for the description of the collision dynamics. Figure 1(b) shows the relevant classical trajectories and the corresponding transition points. One trajectory crosses from the X curve to the B curve on the way in, the other one on the way out. The trajectories start with different impact parameters in order to end up at the same scattering angle.

The optical transition probabilities are governed by dipole factors $\mathbf{d} \cdot \mathbf{E}$, where $\mathbf{d}$ is the vector of the electronic transition dipole moment and $\mathbf{E}$ is the electric field amplitude vector. In the present case the transition is between molecular Σ states, and $\mathbf{d}$ is therefore parallel to the internuclear axis. The axis directions $\mathbf{r}_1$ and $\mathbf{r}_2$ at the transition points are the Condon vectors as shown in the figure. The semiclassical expression for the differential cross section [19] reads

$$\sigma = |p_1 \exp(i\Phi_1)\mathbf{r}_1 \cdot \mathbf{E} + p_2 \exp(i\Phi_2)\mathbf{r}_2 \cdot \mathbf{E}|^2. \quad (2)$$

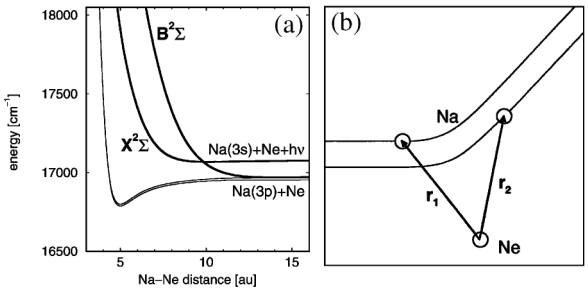

FIG. 1. (a) The potential curves of the NaNe collisional molecule in the light field. Only the $^2\Sigma$ states (heavy lines) participate in the present process. (b) The classical trajectories with the transition points and the Condon vectors.

 0031-9007/04/92(3)/033201(3)$22.50

The relation holds for linear as well as elliptic polarization, where the vector $\mathbf{E}$ is complex. p_1^2 and p_2^2 are classical weight factors and Φ_1 and Φ_2 are the phases for the separate trajectories. Interference oscillations arise because of the variation of the phase with the scattering angle. We introduce vectors $\mathbf{q}_{1,2}$ reciprocal to the Condon vectors such that

$$\mathbf{q}_i \cdot \mathbf{r}_j = \delta_{ij}/p_j \tag{3}$$

and express the electric field as

$$\mathbf{E} = \epsilon_1 \mathbf{q}_1 + \epsilon_2 \mathbf{q}_2. \tag{4}$$

The formula for the cross section simplifies then to

$$\sigma = |\epsilon_1 \exp(i\Phi_1) + \epsilon_2 \exp(i\Phi_2)|^2. \tag{5}$$

Equation (5) shows that the amplitudes and phases of the two interfering terms can be tuned arbitrarily, using ϵ values with corresponding phases and absolute values. Equation (4) shows the way to realize arbitrary complex values for ϵ_1 and ϵ_2.

We measure differential cross sections in a scattering experiment, using two atomic beams and two laser beams. The second laser is part of the detection scheme transferring the Na($3p$) atoms to Rydberg states [20]. The experiments were carried out at a wavelength of 585.611 nm of the excitation laser, i.e., detuned by 120 cm^{-1} above the Na($3s - 3p_{1/2}$) resonance. Scattered Na atoms are registered for different scattering angles. Na velocities after the collision are measured by time of flight and were accepted in a small velocity range only.

Figure 2(b) shows results for two different linear polarization directions of the excitation laser; the polarization is illustrated in Fig. 2(a). In the upper picture both trajectories contribute, leading to pronounced oscillations. In the lower case, $\mathbf{r}_2 \cdot \mathbf{E}$ is close to zero. Only one active trajectory remains, and the interference structure is strongly suppressed.

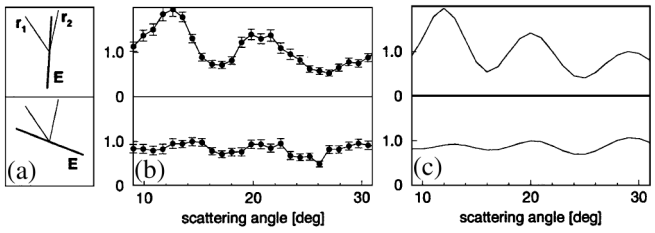

FIG. 2. (a) The linear polarization directions $\mathbf{E}$ used in the experiment and the Condon vectors $\mathbf{r}_1$ and $\mathbf{r}_2$. The relative velocity direction before the collision is along the horizontal axis. (b) The experimental differential cross sections as a function of the scattering angle θ, multiplied by $\sin(\theta)$. Velocity range 1100–1250 m/s. (c) The corresponding theoretical differential cross sections.

Figure 3(b) shows the experimental results for a series of elliptic polarizations as illustrated in Fig. 3(a). We constructed the complex field amplitudes from the requirement $\epsilon_1/\epsilon_2 = \exp(i\phi)$, using the values 30°, 90°, 150°, 210°, 270°, and 330° for the control parameter ϕ. The Condon vectors and p factors were taken from a classical trajectory calculation for the scattering angle 20°. According to Eq. (5), the experimental data are expected to show a continuous shift of the interference pattern. This is indeed observed. The angular positions of the interference maxima increase linearly with the control parameter ϕ. The deviations from linearity have the order of $\pm 0.3°$.

We performed quantum scattering calculations [19], using potential curves by Kerner and Meyer [21] with minor modifications on the basis of previous scattering experiments [22]. The results are shown in Figs. 2(c) and 3(c). The measured and calculated positions of the maxima deviate by less than 0.5° typically. The elliptic polarization experiments were carried out with the same laser intensity $\mathbf{E}^2$ for all values of the control parameter. Following Eqs. (4) and (5), this leads to a considerable variation of the scattered intensity as shown in Fig. 3(b). We use different scales in the graphs to emphasize the regular shift of the interference pattern. Calculated and measured intensities are in good agreement. Following Eqs. (4) and (5) a contrast of 1 is expected, corresponding to zero minimum intensity. This is modified by the finite resolution of the apparatus, which is taken care of in the theoretical curves. The contrast in the theoretical data is

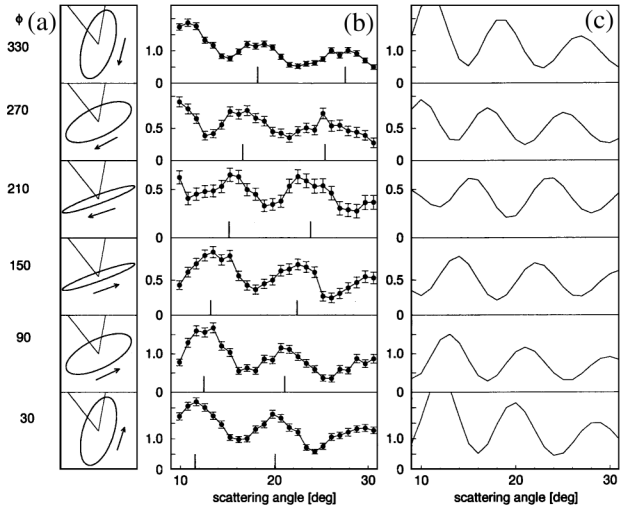

FIG. 3. (a) The elliptic polarization and the Condon vectors for the indicated value of the control parameter. The relative velocity direction before the collision is along the horizontal axis. (b) The experimental differential cross sections as a function of the scattering angle θ, multiplied by $\sin(\theta)$. Velocity range 1150–1300 m/s. The positions of the interference maxima were obtained from a polynomial fit. (c) The corresponding theoretical differential cross sections.

slightly larger compared to the experimental results pointing to some broadening mechanism not fully accounted for in our convolution scheme.

Following Fig. 1(a), our collisional interferometer resembles a Michelson interferometer. Figure 1(b) rather suggests a close analogy to the Young double-slit experiment. The phase difference is indeed for a large part accumulated along the curved trajectories, very similar to the double-slit interferometer. At variance with this interpretation, the light field acts as a beam splitter for the incident atoms which is localized at the Condon radius. Together with Fig. 1(b), this suggests an analogy to a Mach-Zehnder device. The beam splitter plays an active role in the process, unlike in most other interferometers, by transferring phase or amplitude to the wave. It is remarkable that macroscopic matter-wave interferometers have been operated in similar modes [23].

We have demonstrated the control of an atom-atom collision in a polarized laser field. The two interfering collisional waves can be excited with independent complex amplitudes ϵ_1 and ϵ_2. The control is complete, because arbitrary values for each of the amplitudes can be realized using elliptic polarized light. The interference fringes can be shifted to any angular position, and the contrast of the interference pattern can be given any value between 0 and 1. The present experiment requires atomic beams and a differential detector. Similar schemes with beams and integral detection appear possible, for instance, working with a large angular oscillation period. Exploiting the polarization of the exciting laser field appears as a versatile and simple tool for the control of collisional processes.

Support by the Deutsche Forschungsgemeinschaft is gratefully acknowledged.

[1] B. H. Bransden and M. R. C. McDowell, *Charge Exchange and the Theory of Ion-Atom Collisions* (Clarendon, Oxford, 1992).
[2] U. Buck, Adv. Chem. Phys. **30**, 313 (1975).
[3] P. Brumer and M. Shapiro, Chem. Phys. Lett. **126**, 541 (1986).
[4] S. A. Rice and M. Zhao, *Optical Control of Molecular Dynamics* (Wiley, New York, 1999).
[5] R. S. Judson and H. Rabitz, Phys. Rev. Lett. **68**, 1500 (1992).
[6] T. Brixner and G. Gerber, Chem. Phys. Chem. **4**, 418 (2003).
[7] D. Zeidler, T. Hornung, D. Proch, and M. Motzkus, Appl. Phys. B **70**, 125 (2000).
[8] C. Wan, M. Gupta, J. S. Baskin, Z. H. Kim, and A. H. Zewail, J. Chem. Phys. **106**, 4353 (1997).
[9] A. Sanov, S. Nandi, and W. C. Lineberger, J. Chem. Phys. **108**, 5155 (1998); A. Sanov, T. Sanford, S. Nandi, and W. C. Lineberger, J. Chem. Phys. **111**, 664 (1999).
[10] S. C. Zilio, L. Marcassa, S. Muniz, R. Horowicz, V. Bagnato, R. Napolitano, J. Weiner, and P. Julienne, Phys. Rev. Lett. **76**, 2033 (1996); S. R. Muniz, L. G. Marcassa, R. Napolitano, G. D. Telles, J. Weiner, S. C. Zilio, and V. S. Bagnato, Phys. Rev. A **55**, 4407 (1997).
[11] P. Brumer, K. Bergmann, and M. Shapiro, J. Chem. Phys. **113**, 2053 (2000).
[12] M. D. Havey, D. V. Kupriyanov, and I. M. Sokolov, Phys. Rev. Lett. **84**, 3823 (2000); D. V. Kupriyanov, I. M. Sokolov, and A. V. Slavgorodskii, Phys. Rev. A **65**, 063412 (2002).
[13] J. Grosser, O. Hoffmann, and F. Rebentrost, Europhys. Lett. **58**, 209 (2002).
[14] T. Brixner, N. H. Damrauer, G. Krampert, P. Niklaus, and G. Gerber, J. Opt. Soc. Am. B **20**, 878 (2003).
[15] *Atom Interferometry*, edited by P. R. Berman (Academic Press, San Diego, 1997).
[16] T. L. Gustavson, A. Landragin, and M. A. Kasevich, Classical Quantum Gravity **17**, 2385 (2000).
[17] J. Schmiedmayer, M. S. Chapman, C. R. Ekstrom, T. D. Hammond, S. Wehinger, and D. E. Pritchard, Phys. Rev. Lett. **74**, 1043 (1995).
[18] R. Dumke, T. Müther, M. Volk, W. Ertmer, and G. Birkl, Phys. Rev. Lett. **89**, 220402 (2002).
[19] F. Rebentrost, S. Klose, and J. Grosser, Eur. Phys. J. D **1**, 277 (1998).
[20] J. Grosser, O. Hoffmann, and F. Rebentrost, in *Atomic and Molecular Beams*, edited by R. Campargue (Springer, Berlin, 2001), p. 485.
[21] C. Kerner, Ph.D. thesis, Universität Kaiserslautern, 1995; C. Kerner and W. Meyer (to be published).
[22] J. Grosser, O. Hoffmann, and F. Rebentrost, J. Phys. B **33**, L577 (2000).
[23] H. Hinderthür, A. Pautz, F. Ruschewitz, K. Sengstock, and W. Ertmer, Phys. Rev. A **57**, 4730 (1998).